Nanoscale

Accepted Manuscript

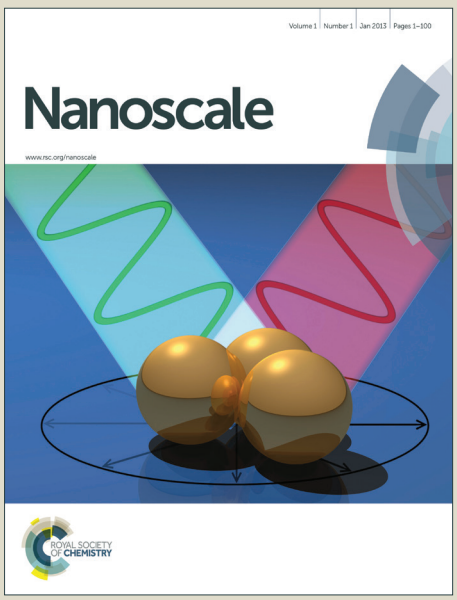

ROYAL SOCIETY OF CHEMISTRY

www.rsc.org/nanoscale

Reducing ZnO Nanoparticle Cytotoxicity by Surface Modification

Mingdeng Luo[1], *Cenchao Shen*[2], *Bryce N. Feltis*[2, 3], *Lisandra L. Martin*[1], *Anthony E. Hughes*[4], *Paul F.A. Wright*[2], *Terence W. Turney*[3*]

[1]School of Chemistry, Monash University, Clayton VIC 3800, Australia, [2]School of Medical Sciences, and NanoSafe Australia, RMIT University, Bundoora VIC 3083, Australia, [3] Department of Materials Engineering, Monash University, Clayton VIC 3800, Australia and [4] CSIRO, Materials Science and Engineering, Clayton VIC 3168, Australia.

* Corresponding author, Phone: +61 3 9905 1762, Fax: +61 3 9905 4940, E-mail: terry.turney@monash.edu

Abstract:

Nanoparticulate zinc oxide (ZnO) is one of the most widely used engineered nanomaterials and its toxicology has gained considerable recent attention. A key aspect for controlling biological interactions at the nanoscale is understanding the relevant nanoparticle surface chemistry. In this study, we have determined the disposition of ZnO nanoparticles within human immune cells by measurement of total Zn, as well as the proportions of extra- and intracellular dissolved Zn as a function of dose and surface coating. From this mass balance, the intracellular soluble Zn levels showed little difference in regard to dose above a certain minimal level or to different surface coatings. PEGylation of ZnO NPs reduced their cytotoxicity as a result of decreased cellular uptake arising from a minimal protein corona. We conclude that the key role of the surface properties of ZnO NPs in controlling cytotoxicity is to regulate cellular nanoparticle uptake rather than altering either intracellular or extracellular Zn dissolution.

Keywords: ZnO nanoparticles, surface chemistry, PEGylation, cell uptake, cytotoxicity

Introduction

Although applications of nanoparticles (NPs) are growing exponentially, research into their toxicological impact and possible long-term hazards to human health and the environment is still relatively undeveloped.[1] Zinc oxide (ZnO) NPs are one of the most commonly used engineered nanomaterials in personal care products, such as sunscreens, owing to their excellent UV attenuation properties in the region just below 400 nm The nanotoxicology of ZnO NPs has been intensively studied and most reports conclude that cellular toxicity is controlled in part by intracellular dissolution of the NPs to afford readily bioavailable, but generally uncharacterised, smaller Zn species, usually assumed to be Zn^{2+}.[2-6] Some studies on the toxicity of ZnO NPs have shown a dose-dependent cytotoxicity to a number of different cells,[7] with NP-induced oxidative stress also playing a central role in cytotoxicity.[8-10]

While the work to date has been substantial, precise NP dissolution mechanisms and how these affect the cytotoxicity of ZnO nanoparticles remains unclear. Critical to this process are the surface characteristics of the NPs, which are of particular importance in NP-biological interactions.[11, 12] In this study, we have undertaken an examination of the effects of ZnO NP surface modification upon NP cellular transport. Adding additional complexity, as soon as NPs enter into the human body, their surface chemistry will be modified by biological fluids, such as blood and serum. Thus, numerous studies have observed formation of a protein corona on the surface of the NPs.[13-15] It has also been shown that the phosphate and carbonate ions present within serum will react with both ZnO nanoparticles and any solubilised Zn to form a complex mixture of species with varying solubility.[16, 17] During circulation, the protein-corona decorated NPs or their secondary products can be taken up into cells via several different endocytosis pathways, involving active or passive transport.[18,19] When ZnO NPs are subject to endocytosis, dissolution is likely as ZnO NPs are unstable in the low pH (ca 4.0) conditions encountered in the lysosome and late endosome

(pH 5.5), which can result in the release of bioavailable zinc at potentially cytotoxic levels. Efforts have been made to prevent ZnO NP dissolution through modification processes such as iron doping, which has notably reduced the toxicity of ZnO NPs towards rodent lung and zebrafish embryos.[20] Whilst iron doping appeared to slow the rate of particle dissolution, it did not alter their uptake characteristics. Recent reports indicate that the cytotoxicity of ZnO NPs is independent of the amount of extracellular soluble Zn in the cell culture medium and that direct nanoparticle contact with the cells is important.[21-23] As NP uptake appears to be a critical requirement for ZnO NP cytotoxicity,[8, 24] lattice doping of ZnO nanoparticles will only afford at best a partial solution to the safe design of engineered nanomaterials.[25] A more effective strategy in reducing ZnO NP cytotoxicity would be to inhibit both NP uptake into cells and their subsequent dissolution. In particular, uptake may also be sensitive to modification of the surface protein corona, and reduction in the formation of the protein corona, could reduce possible uptake pathways of NPs into cells.[14, 26, 27] Conversely, it has also been reported that the presence of the protein in foetal calf serum can result in a substantial decrease in the cytotoxicity of ZnO NPs towards human lung epithelial cells.[28] These contradictory studies demonstrate both the complexity of the surface protein corona and our currently limited understanding of how the corona interacts with the cellular surface.

Polyethylene glycols (PEGs) have been widely used in biological and medical applications, such as for drug delivery, because of their excellent biocompatibility and biodegradation properties.[29] It has been reported that PEGylation of nanoparticles is very effective in inhibiting the nonspecific binding of NPs to blood proteins and macrophages.[30] PEGylation of NP surfaces, by chemical grafting of a PEG-containing moiety, appears to afford a more refractory coating compared with the PEG which is physically adsorbed and thus such PEGylated NPs should also possess a longer blood circulation half-life.[31] Recently, PEGylated

2 nm ZnO quantum dots (QDs) have demonstrated intracellular uptake and have been used to label a variety of cells, including stem cells, with low cytotoxicity at a low dose (30ppm).[32]

In the current study, we have investigated the influence of surface chemistry on the cytotoxicity of ZnO NPs towards human THP-1 immune cells (both monocyte and macrophage-like cells), in order to understand: (1) the relationship between surface properties and cytotoxicity of ZnO NPs in *in vitro* cell studies; (2) how cytotoxicity is related to ZnO dissolution and the formation of a protein corona; and (3) which of these is the stronger determinant for the cytotoxicity of ZnO NPs. We have investigated the dissolution of ZnO NPs in several different biologically relevant matrices and examined the effects of surface coatings on protein corona formation by quantifying the total protein load absorbed onto the particle surface. We were also able to correlate protein corona formation with the surface chemistry modification of the ZnO NPs.

Materials and methods

Materials

ZnO NPs (particle size = 39 ± 4 nm; wurtzite structure; BET surface area = 27.2 m^2/g), were identical in properties to an OECD standard reference nanomaterial, NM-112[33] and were available through the manufacturer, Micronisers Australasia Pty Ltd, Dandenong, Victoria, Australia. Tetraethyleneglycol monomethyl ester (MTEG), 3-(triethoxysilyl) propyl isocyanate (TESPIC) and 3-aminopropyltriethoxysilane (APTES) were obtained from Sigma-Aldrich and used without further purification.

Surface modification of ZnO NPs

Surface modified ZnO NPs were synthesized according to the literature with minor alterations to the procedure.[34] A typical procedure for the synthesis of APTES modified ZnO

NPs (denoted as ZnO@APTES NPs) was as follows; 2 g of ZnO NPs were dispersed into 200 mL anhydrous toluene under nitrogen gas flow in a 250 ml round bottom flask. After 1 h of magnetic stirring, 1 mL of APTES was added under nitrogen protection. The mixture was refluxed under a nitrogen gas flow for a further 15 h. Finally, after cooling down to room temperature, the reactant was centrifuged (2,500 x *g*) and washed 3 times using fresh toluene and anhydrous ethanol to remove the excess APTES, then dried in a vacuum oven overnight (80^{o}C) to remove the solvent. The synthesis and characterization of *N*-[3-(triethoxysilyl)propyl]-3,6,9,12-tetraoxatridec-1-yl ester of carbamic acid, (PEGSi) and ZnO@PEG NPs are reported in the Supplementary Information, as are the instrumental methods used in the characterization of modified ZnO NPs.

ZnO NP solubility determination

NP solutions were incubated in water, cell culture media (with or without 10% v/v fetal bovine serum), or artificial lysosomal fluid (ALF).[35] The solubility of ZnO NPs in different media was determined by ultracentrifugation of the supernatant liquid through a membrane and Zn levels determined via Inductively Coupled Plasma (ICP) Time of Flight (TOF) Mass Spectrometry (MS) as follows: After incubation for 24 hours at 37^{o}C, NP-containing suspensions were centrifuged through 3 kDa membrane filters (Microcon YM-3 filter, Millipore, USA) at 13,500 x *g* for 60 min. Each solution was then diluted with ~3 vol% double distilled nitric acid in ultra-pure (Milli-Q) water (40 mL). For drift correction, an internal standard of indium was added to each solution (at 30 ppb, diluted from a commercial stock solution). Solutions were then measured with a GBC Optimass 9500 ICP-TOF-MS instrument. Commercial stock solutions of Zn were used for calibration standards (~10, 30, 70, and 100 ppb). All standards were ionic-strength adjusted, so as to contain the same concentration of nitric acid present in the samples.

Cell culture and cytotoxicity assay

A human acute monocytic leukaemia cell line (THP-1) was cultured in RPMI-1640 media containing 10% v/v foetal bovine serum (FBS), 100 ml/L gentamycin, 4.5 g/L glucose, 1 mM pyruvate, 0.05 M 2-mercaptoethanol and 2 mM L-glutamine supplementation. Cells were maintained in a humidified incubator at 37^{o}C and 5% CO_2. Cells were centrifuged and re-suspended in fresh media before seeding in 96-well plates at 10^5 cells per well. One hour later, ZnO NPs suspended in tissue culture media (conditioned for 24 h), were added for a final concentration of 10–100 µg/mL in a final incubation volume of 200 µL. Macrophage-like cells were differentiated from THP-1 monocytes by incubating 8×10^4 cells per well (allowing some cell growth in 24 h and thus arriving at the same approximate cell number as the monocytes) with 20 nM phorbol-12-myristate-13-acetate (PMA) for 24 h. After which the media was aspirated off and fresh media containing NPs at a concentration of 10–100 µg/mL was added. After 20 h, MTS (CellTiter 96® aqueous kit, Promega, Madison, WI, USA) was added to each well and incubated for 4 h before being measured at 490 nm on a plate reader (FlexStation 3, Waltham, MA, USA). Wells containing the concentration range of NPs and MTS reagent alone were used to control for any direct optical density effects of NPs, by subtracting these values from the experimental readings. Each treatment was performed in triplicate wells for three individual experiments.

Measurement of total intracellular Zn levels

Solutions from the cell culture experiments were characterized for total zinc concentration per cell via ICP-MS following the method described above for solubility determinations. Prior to the extraction, cells were washed 3 times in fresh cell culture media to remove extracellular nanoparticles. Each well was then washed twice (2 x 200 µL) with double-distilled concentrated nitric acid, in order to disrupt the cells and solubilise all Zn present. After dilution with ~3 vol% double-distilled nitric acid in ultra-pure (Milli-Q) water (40 mL),

each sample solution was filtered via a 0.45 µm nylon syringe filter to prevent blockage of the ICP-MS nebuliser. Zinc levels in the filtered solutions were then measured with an ICP-TOF-Mass Spectrometry (GBC Optimass 9500).

Intracellular zinc ion measurement

Intracellular zinc ions were measured by zinquin ethyl ester (Biotium, CA, USA), a UV excitable fluorescent zinc indicator (Ex 364 nm/Em 385 nm).[36] Cells were seeded in 96-well plates and incubated with ZnO NPs for 24 h as described above for the cell culture procedure. After 24 h co-culture with NPs, cells were washed with phosphate-buffered saline (PBS) to remove extracellular zinc. Cells were then incubated with zinquin ethyl ester (100 µL, 25 µM) for 30 min in a dark and humidified incubator at 37^{o}C and 5% CO_2 to allow for cellular uptake. Once the zinquin ethyl ester was internalized, its ethyl ester group is cleaved by cytosolic esterases which impede its efflux across the plasma membrane. After 30 min, the cells were washed again with PBS to remove extracellular zinquin ethyl ester. Finally, fresh media was added and cells were analysed using flow cytometry (FACS Canto II, Becton, Dickinson and Co., Franklin Lakes, NJ, USA). Cells were designated as "zinquin positive" (high zinc ion levels) when zinquin expression was greater than the 95th percentile of the normal distribution of zinquin in the untreated control population, ie. "zinquin negative" (low zinc ion levels). Each treatment was performed in triplicate for each of three experiments.

Protein assay and protein-related zinc determination

The amount of protein bound to ZnO NP surface was measured by the bicinchoninic acid (BCA) assay.[37] Prior to the assay, NPs were dispersed into RPMI-1640 medium containing 10% v/v FBS at concentrations of 10–100 µg/mL, and incubated at 37^{o} C for 24 h in a mixing incubator with a shaking speed of 220 rpm. After incubation, an aliquot (1 mL) was centrifuged down at 17000 x *g* for 10 min, washed with PBS buffer twice to remove free

protein and finally resuspended in 1 mL of PBS solution. For the BCA assay, 100 µL of sample was mixed with 100 µL of BCA and incubated for 30 min at room temperature before the optical absorbance was measured (at 490 nm) using a plate reader (BioTek ELX808IU, Winooski, VT, USA). A standard curve was obtained by measuring known concentrations of bovine serum albumin (BSA) solution. After the assay, samples were dissolved with 200 µL double-distilled concentrated nitric acid and total Zn levels determined as above by ICP-MS. These total zinc levels were used to calculate the amount of protein per NP. Each treatment was performed in duplicate. To control for potential interference with the assay, ZnO NPs alone were tested for optical absorbance at 490nm, which was found to be negligible (see Supplementary Information Figure S1).

Results

Synthesis and characterization of surface modified ZnO NPs

Surface modification of ZnO NPs was achieved by silanization using a grafting method with substituted trialkoxysilanes on the naturally hydroxylated and partially carbonated ZnO NP surfaces. Prior to biological testing, the surface modified NPs were characterized spectroscopically. Fourier transform infrared (FTIR) spectra confirmed that the silanisation reactions between ZnO and the coating agents were successful (see Supplementary Information Figure S2). The capping agents were adsorbed onto the ZnO surface through Zn–O–Si bonds. Compared to bare ZnO NPs, the modified ZnO NPs exhibited characteristic peaks for the corresponding ligands. Scanning electron microscopy (SEM) was applied to characterize the primary particle size and morphology of each grafted ZnO NP (Figure S3). Analysis of these SEM images revealed monodispersed hexagonal ZnO NPs with a diameter of around 40 nm. No substantial differences in particle morphology of the samples were observed in the SEM. Powder X-ray diffraction (XRD) spectra confirmed that the ZnO NPs had a hexagonal wurtzite type crystal structure both before and after surface modification

(Figure S4).

X-ray photoelectron spectroscopy (XPS) was used to study the surface composition of modified NPs. The XPS binding energies of bare and surface modified ZnO NPs are presented in Table S2. In particular, the Si 2p binding energy is typical for Si^{4+} in siloxanes and lower than the binding energy for SiO_2 (Figure S4 and S5). Comparison of the Si/Zn atomic ratios from the XPS suggest that there is about twice as much surface silanization in the ZnO@APTES than for the ZnO@PEG sample (Table S3).

The surface charges of the different ZnO NPs in water were determined by measurement of zeta potential as a function of pH (Figure 1). Bare ZnO NPs had an isoelectric point (IEP) at about 9.1, while the IEPs of PEGylated ZnO and amino-modified ZnO NPs were 8.2 and >10 respectively. Furthermore, all the NPs were positively charged at physiological pH (7.4) in water. Estimates of the Si/Zn ratio independently derived from XPS, XRF and TGA data showed that the extent of silanization in the case of ZnO@APTES was about double that of ZnO@PEG (see Supplementary Information).

Cytotoxicity of ZnO NPs

The cytotoxicity of the bare and modified ZnO NPs was tested with human THP-1 immune cells (with both monocytes and macrophages). In these experiments, THP-1 immune cells were exposed to ZnO NPs at concentrations of 10, 50, and 100 μg/mL. All ZnO nanoparticles showed a dose dependent cytotoxicity (Figure 2). Both bare ZnO NPs and APTES-modified ZnO exhibited a similar cytotoxicity. In the case of monocytes, PEGylation significantly reduced the cytotoxicity of ZnO NPs at all doses treated, being half as cytotoxic as bare ZnO NPs at both 50 and 100 μg/mL. In the case of macrophages, all ZnO NPs were not cytotoxic at the lowest dose (10 μg/mL), while at concentrations of 50 μg/mL, PEGylated ZnO NPs exhibited markedly reduced cytotoxicity compared to both uncoated and APTES-modified

ZnO NPs; at 100 μg/mL, all NPs caused very low cell viability.

Cell-Associated Zinc

The total cell-associated zinc derived from the ZnO NPs was determined by ICP-MS and presented as an average mass of zinc per cell (Table 1). This data showed that very high levels of zinc were present in all cells at NP concentrations of 50 μg/mL and provides an upper limit for intracellular zinc level, if it is assumed that there are relatively few ZnO NPs adsorbed on the external cell membrane. Indeed, a previous synchrotron-based X-ray fluorescence microscopy study, using the present unmodified ZnO NPs has not shown any appreciable concentration of membrane-adsorbed Zn associated with these cells.[38] The total cell-associated Zn in macrophages was about twice that of monocytes for the bare and modified ZnO NP-treated cells. Moreover, the total Zn from PEGylated ZnO NP-exposed cells was much less than for bare and APTES-modified ZnO, being over an order of magnitude lower for both monocytes and macrophages, suggesting that the cellular uptake of PEGylated ZnO NPs was significantly less.

The intracellular dissolution of ZnO NPs was determined by using a specific fluorescent zinc ion indicator, zinquin ethyl ester.[6] The number of monocyte and macrophage cells, containing high levels of intracellular zinc, increased gradually with increasing ZnO NP doses (Figure 3). More interestingly, PEGylated ZnO NPs showed the lowest level of intracellular Zn ions when compared to both bare and APTES-modified ZnO NPs at concentrations of 10 and 50 μg/mL, in both monocytes and macrophages. The levels of intracellular soluble Zn in the controls (cells without ZnO NP treatment) were negligible, and below the limit of instrument detection. At high NP concentrations (100 μg/mL), PEGylated ZnO NP-exposed cells still showed slightly lower intracellular zinc levels in comparison to bare ZnO NPs, while Zn ions released from ZnO@APTES NPs were similar to those from bare ZnO NPs.

Solubility of ZnO NPs

The solubility of ZnO NPs in different biological media was investigated by membrane ultracentrifugation followed by ICP-MS to determine the zinc concentration in solution. We found that the aqueous solubility of modified ZnO NPs did not change significantly when particles were incubated in cell culture medium (Table 2). In the presence of serum, the solubility of the NPs was slightly lower than that in the pure culture medium. However, when the NPs were incubated with artificial lysosomal fluid (ALF, see the Supplementary Information Table S4 for its composition), a solution at the much lower pH of 4.5 that mimics conditions after cellular uptake, all ZnO NPs were almost completely dissolved.

Zinc mass balance in NP-treated cells

The above data enable an estimation of the mass balance for NP-derived Zn. The residual unreacted extracellular ZnO was estimated by subtraction of the extracellular soluble Zn and the intracellular total Zn from the initial mass of Zn added as ZnO NPs. Similarly, the mass of intracellular ZnO NPs was derived from subtraction of the zinquin complexed Zn from the total intracellular Zn. Table 3 represents the mass balance of added ZnO NPs in macrophages at the highest concentration (100 μg/mL). We found that most of the total added ZnO remained unreacted, being ~90% for bare and ZnO@APTES, and 98.5% for ZnO@PEG NPs. More importantly, the intact intracellular ZnO NPs in ZnO@PEG-exposed cells was less than 10% of that in bare ZnO and ZnO@APTES NP-exposed cells. On the other hand, there is little difference for the dissolved intracellular zinc and dissolved extracellular zinc with the differently coated NPs.

Quantification of protein binding onto ZnO NPs

To determine the magnitude of total protein adsorption onto the ZnO NPs within the culture media, NP-associated protein assays were undertaken, by incubating NPs with RPMI-1640

medium containing 10% v/v FBS and washing with fresh PBS solution to remove the unadsorbed protein components (Table 4). The amino-modified ZnO NPs were found to absorb twice as much proteinaceous material than the bare ZnO NPs. On the contrary, ZnO@PEG NPs had a very low protein binding, with only about 40% of the amount of protein adsorbed as for bare ZnO NPs.

Discussion

The surface chemistry of nanoparticles is of particular importance in their interaction with biological systems. In this study, we investigated how modification of the surface properties of nanomaterials alters their biological fate by comparing differences between samples of a well characterised ZnO NP, which had different types of coatings chemically grafted onto it. In particular, polyethylene glycol (PEG) has been widely used in biological and medical applications, such as for drug delivery, because it confers excellent biocompatibility. The PEGylation of nanoparticles can be achieved either by physical adsorption or by covalent attachment.[39, 40] Compared to physically adsorbed PEG, covalently PEGylated nanoparticles, such as those used in this study, are more likely to retain their PEG coating during any intermediate dissolution of the NP. Similarly, 3-aminopropyltriethoxysilane (APTES), which has been frequently used to modify metal and metal oxide nanoparticles,[34, 41] was also used here to surface graft functional amino groups. In effect, this gave us a “low fouling, highly biocompatible” surface in the ZnO@PEG NPs and a “high fouling, poorly biocompatible” surface in the ZnO@APTES NPs.

The cytotoxicity profiles of the covalently coated and uncoated ZnO NPs were assessed for human THP-1 immune cells, including monocytes and THP-1-derived macrophages. Macrophages are likely to be among the first immune cells to encounter NPs and their phagocytic function will likely result in higher intracellular NP exposure concentrations than

for monocytes or other cell types. It was found that the cytotoxicity of PEGylated ZnO NPs was lower than for uncoated ZnO NPs, even at the highest concentration (i.e. at 100 µg/mL, Figure 2). However, in the case of ZnO@APTES , despite its high fouling nature, similar cytotoxicity to uncoated ZnO at all exposure concentrations was observed. In previous work,[7, 42] the cytotoxicity of ZnO NPs has been largely attributed to the release of Zn ions resulting from partial dissolution of the NPs in either the extracellular or intracellular matrix. However, the main contributor to this process has been shown to be intracellular dissolution and that extracellular dissolution of ZnO NPs, at least in the presence of serum proteins, plays at best a minor role in overall cytotoxicity.[6,38] Hence, cellular uptake becomes a critical determinant of cytotoxicity. It is possible that the decreased cytotoxicity of PEGylated ZnO relative to that of the uncoated NPs, as observed in the current study, could be due to either reduced uptake resulting from hydrostatic repulsion of the highly aqueous PEG and the lipid bilayer of the cell surface, or to reduced dissolution after uptake, arising from limited accessibility of the NP surface to the low pH endosomal components.

The coated and uncoated NPs used in this study showed differences in solubility in various biologically-relevant media. Thus, the solubilities of ZnO NPs in both water and cell culture medium were found to be low, regardless of the surface coatings (Table 2). Addition of serum decreased their solubility slightly, suggesting some protein-bound Zn was trapped on the NP side of the centrifugal filter, which otherwise would have been in solution in the protein-free system.[28, 43] These findings were similar, but slightly different to our previous work using different methodology, where the Zn analyses were performed after extensive dialysis, rather than by filtration, in which we found that any soluble zinc ions rapidly form poorly soluble zinc-phosphate-carbonate NPs in the presence of cell culture media and serum.[17] In the intracellular environment, endosomal pHs range from 6 in the early endosomes, to 4 in lysosomes.[44] ZnO would be expected to be quite unstable at such low pH ranges.

Intracellular dissolution would be likely as a consequence of endosomal/lysosomal fusion after phagocytosis . Indeed, our assessment of this dissolution process using the solubility of ZnO NPs in an artificial lysosomal fluid (at pH 4.5), found that all NPs were almost completely dissolved. Although the ALF present in this system is very much in excess when compared to the very small volume present intracellularly, it is surprising that no significant differences in solubility were observed between the coated and uncoated ZnO NPs. These similarities in solubility suggest that the observed large differences in cytotoxicity were not well-correlated with intracellular NP dissolution, leaving NP uptake as a more likely source of the variation in cytotoxicity observed with the different coatings.

We have previously correlated cytotoxicity of ZnO NPs to both intracellular Zn^{2+} ions as well as intracellular reactive oxygen species (ROS) generation; uncoated ZnO NP induced cytotoxicity was strongly correlated with free intracellular zinc ions in human immune cells (R^2=0.945).[6] In the present study, we find that the cytotoxicity of surface modified ZnO NPs could similarly be correlated to intracellular zinc concentration (Figure 4). The highest zinc concentrations were measured in ZnO and ZnO@APTES NP-exposed cells, far higher than the zinc levels in cells exposed to ZnO@PEG NPs (Figure 3). As there appeared to be little difference in solubility in ALF for these materials, it is likely that differences in uptake were leading to higher intracellular zinc concentrations, leading to increased induction of oxidative stress, and ultimately cell death by both apoptosis and necrosis.[45] The total cell-associated zinc concentration would also seem to support this hypothesis, with zinc from the PEGylated ZnO NPs being lowest by a very large margin, amongst the three particulates (Table 1). It is significant that the total cell-associated zinc concentrations in the uncoated and ZnO@APTES NP-treated cells were much higher than the intracellular Zn^{2+}, suggesting that the bulk of the ZnO NPs taken up by these cells remains undissolved and that the small amount that does dissolve is sufficient to induce cytotoxicity. We also cannot discount that some extracellular

ZnO NPs may become trapped or stuck to cells during the washing process, so this total zinc figure could be overestimated. However, neither Gilbert and co-workers nor we have observed any appreciable concentrations of membrane adherent ZnO NP in such experiments.[5, 38] Use of ZnO@PEG NPs enabled the correlation between cytotoxicity and zinc to be examined at much lower intracellular concentrations. Figure 4 shows substantial deviations from linearity at low Zn concentrations, presumably resulting from efficient Zn clearance from the cells at such low concentrations.

The zinc mass balance demonstrates a number of important insights into how these cells handle both ZnO NPs and zinc homeostasis more generally. Extracellular, soluble zinc levels reached approximately 11.9 µM (Table 3), whereas intracellular soluble zinc was cytotoxic to all cells at 2.9 µM, a finding consistent with Canzoniero *et al*., who postulated that intracellular zinc levels above 1 µMµM tend to induce cytotoxicity in neuronal cells.[46] The immune cells used in this study would be expected to have, and appear to demonstrate, a slightly higher tolerance to excess zinc. From previous studies[17] we have observed that extracellular soluble zinc is unable to induce cytotoxicity, which shows that even with very high extracellular concentrations, the cells are able to regulate intracellular zinc ion levels sufficiently to prevent cytotoxicity. However, once ZnO NPs enter the cells, the increased ZnO solubility within the endosomal compartments (Table 2) results in large increases in intracellular zinc and, if uptake was sufficient, in cytotoxicity. In ZnO and ZnO@APTES N-treated cells, intact intracellular NPs were present at very high concentration and correlate with the cytotoxicity of these materials. However, lower cytotoxicity of ZnO@PEG-treated appears arise from reduced NP uptake.

To explain the observed reduction in uptake of PEGylated ZnO NPs and their significantly lower cytotoxicity, compared to the high levels of uptake for bare and APTES-modified ZnO

NPs, we must look to the mechanisms of NP uptake. NPs are usually taken up by cells via endocytosis,[47] a process that may be highly dependent on proteins that bind to the surface of the NPs and form a protein-NP corona. This corona can alter the properties of the NPs and therefore needs to be taken into account when characterizing the biological interactions of NPs.[48] It has been reported that PEGylation is very effective in inhibiting the nonspecific binding of NPs to proteins. In our study, we found that the protein binding ability of PEGylated ZnO NPs was half as much as the bare ZnO NPs (Table 4). As predicted, ZnO@APTES can bind a greater quantity of protein, which is attributed to its highly positively-charged aminated surface. It may be that this decreased protein binding of PEGylated ZnO NPs inhibits the formation of a protein corona around the ZnO@PEG NPs, which then decreases the uptake of such NPs into cells. Interestingly, the more extensive protein corona of APTES-modified ZnO NPs did not help to increase cellular uptake. It has been reported that the protein "hard corona" around NPs changes significantly in terms of the amount of bound protein, but not in protein composition, over time.[15, 48-50]

The role of protein binding in relation to PEG is subtle, and complex, and depends on the nature of the bound proteins and the receptors. Thus, we cannot discount that it may be the binding kinetics of specifically bound proteins, and not simply the total amount of bound protein, that may be the critical determinant for NP cellular uptake.

Conclusions

We have successfully synthesized surface modified ZnO NPs through surface grafting and demonstrated that the surface chemistry of NPs played a vital role in determining their cytotoxicity. PEGylation of ZnO NPs reduced their cytotoxicity, resulting from a decrease in cellular uptake, while the APTES-modified ZnO NPs showed similar cytotoxicity to bare materials. Determination of extra- and intracellular ZnO NP levels and the extent of their solubilisation has enabled an approximate materials flow analysis for the added ZnO NPs. No

significant differences for the intracellular dissolution of modified ZnO NPs were observed, suggesting that the cellular uptake of ZnO NPs, possibly influenced by protein corona, is a much more important determinant for ZnO cytotoxicity.

Conflict of interest

The authors report no conflicts of interest, except for TWT who is also Chief Technical Officer of Micronisers Australasia Pty Ltd, a manufacturer of ZnO NPs. The authors alone are responsible for the content and writing of the paper.

Acknowledgements

The financial support from National Health and Medical Research Council (NHMRC) project (#616621) and Advanced Manufacturing Cooperative Research Centre (AMCRC) is gratefully acknowledged. The authors would like to thank Micronisers Pty Ltd for supply of ZnO nanoparticles, Dr Massimo Raveggi at Monash University for assistance with ICP-MS, Thomas Gengenbach for XPS analysis and Steve Peacock at CSIRO for assistance with XRF analysis. ML was supported by Monash University Faculty of Science Dean's International Postgraduate Research Scholarship.

References

1 A. Elsaesser and C. V. Howard, Adv. Drug Deliv. Rev., 2012, **64**, 129.

2 S. W. Y. Wong, P. T. Y. Leung, A. B. Djurišić and K. M. Y. Leung, Anal. Bioanal. Chem., 2009, **396**, 609.

3 W. S. Cho, R. Duffin, S. E. Howie, C. J. Scotton, W. A. H. Wallace, W. MacNee, M. Bradley, I. L. Megson and K. Donaldson, Particle and Fibre Toxicology, 2011, **8**, 27.

4 M. Prach, V. Stone and L. Proudfoot, Toxicol. Appl. Pharmacol., 2013, **266**, 19.

5 B. Gilbert, S. C. Fakra, T. Xia, S. Pokhrel, L. Madler and A. E. Nel, ACS Nano, 2012, **6**, 4921.

6 C. Shen, S. A. James, M. D. de Jonge, T. W. Turney, P. F. A. Wright and B. N. Feltis, Toxicol. Sci., 2013, **136**, 120.

7 X. Deng, Q. Luan, W. Chen, Y. Wang, M. Wu, H. Zhang and Z. Jiao, Nanotechnology, 2009, **20**, 115101.

8 T. Xia, M. Kovochich, M. Liong, L. Madler, B. Gilbert, H. Shi, J. I. Yeh, J. I. Zink and A. E. Nel, ACS Nano, 2008, **2**, 2121.

9 B. De Berardis, G. Civitelli, M. Condello, P. Lista, R. Pozzi, G. Arancia and S. Meschini, Toxicol. Appl. Pharmacol., 2010, **246**, 116.

10 V. Sharma, D. Anderson and A. Dhawan, J. Biomed. Nanotechnol., 2011, **7**, 98.

11 A. Verma and F. Stellacci, Small, 2010, **6**, 12.

12 A. E. Nel, L. Mädler, D. Velegol, T. Xia, E. M. Hoek, P. Somasundaran, F. Klaessig, V. Castranova and M. Thompson, Nat. Mater., 2009, **8**, 543.

13 D. Walczyk, F. B. Bombelli, M. P. Monopoli, I. Lynch and K. A. Dawson, J. Am. Chem. Soc., 2010, **132**, 5761.

14 I. Lynch and K. A. Dawson, Nano Today, 2008, **3**, 40.

15 M. Lundqvist, J. Stigler, G. Elia, I. Lynch, T. Cedervall and K. A. Dawson, Proc. Natl. Acad. Sci. U.S.A., 2008, **105**, 14265.

16 R. B. Reed, D. A. Ladner, C. P. Higgins, P. Westerhoff and J. F. Ranville, Environ. Toxicol. Chem., 2012, **31**, 93.

17 T. W. Turney, M. B. Duriska, V. Jayaratne, A. Elbaz, S. J. O'Keefe, A. S. Hastings, T. J. Piva, P. F. A. Wright and B. N. Feltis, Chem. Res. Toxicol., 2012, **25**, 2057.

18 Y. Mosesson, G. B. Mills and Y. Yarden, Nat. Rev. Cancer, 2008, **8**, 835.

19 T. G. Iversen, T. Skotland and K. Sandvig, Nano Today, 2011, **6**, 176.

20 T. Xia, Y. Zhao, T. Sager, S. George, S. Pokhrel, N. Li, D. Schoenfeld, H. Meng, S. Lin, X. Wang, M. Wang, Z. Ji, J. I. Zink, L. Madler, V. Castranova and A. E. Nel, ACS Nano, 2011, **5**, 1223.

21 P. J. Moos, K. Chung, D. Woessner, M. Honeggar, N. S. Cutler and J. M. Veranth, Chem. Res. Toxicol., 2010, **23**, 733.

22 B. N. Feltis, S. J. O'Keefe, A. J. Harford, T. J. Piva,T. W. Turney and P. F. A. Wright, Nanotoxicology, 2012, **6,** 757.

23 M. Xu, J. Li, N. Hanagata, H. Su, H. Chen and D. Fujita, Nanoscale, 2013, **5**, 4763.

24 R. Roy, A. Tripathi, M. Das and P. D. Dwivedi, J Biomed Nanotechnol, 2011, **7**, 110.

25 A. E. Nel, Science, 2006, **311**, 622.

26 A. A. Shemetov, I. Nabiev and A. Sukhanova, ACS Nano, 2012, **6**, 4585.

27 S. Chakraborti, P. Joshi, D. Chakravarty, V. Shanker, Z. A. Ansari, S. P. Singh and P. Chakrabarti, Langmuir, 2012, **28**, 11142.

28 I. L. Hsiao and Y. J. Huang, J. Nanopart. Res., 2013, **15**, 1.

29 R. B. Greenwald, Y. H. Choe, J. McGuire and C. D. Conover, Adv. Drug Deliv. Rev., 2003, **55**, 217.

30 A. S. Karakoti, S. Das, S. Thevuthasan and S. Seal, Angew. Chem. Int. Ed., 2011, **50**, 1980.

31 Q. He, J. Zhang, J. Shi, Z. Zhu,L. Zhang, W. Bu, L. Guo and Y. Chen, Biomaterials, 2010, **31**, 1085.

32 S. H. Hsu, Y. Y. Lin, S. Huang, K. W. Lem, D. H. Nguyen and D. S. Lee, Nanotechnology, 2013, **24**, 475102.

33 C. Singh, S. Friedrichs, M. Levin, R. Birkedal, K. Jensen, G. Pojana, W. Wohlleben, S. Schulte, K. Wiench and T. Turney, EUR Report, 2011, 25066.

34 F. Grasset, N. Saito, D. Li, D. Park, I. Sakaguchi, N. Ohashi, H. Haneda, T. Roisnel, S. Mornet, and E. Duguet, J. Alloys Compd., 2003, **360**, 298.

35 Y. Hedberg, J. Gustafsson, H. L. Karlsson, L. Möller and I. Wallinder, Particle and Fibre Toxicology, 2010, **7**, 23.

36 P. Coyle, P. D. Zalewski, J. C. Philcox, I. J. Forbes, A. D. Ward, S. F. Lincoln, I. Mahadevan and A. M. Rofe, Biochem. J., 1994, **303**, 781.

37 P. Smith, R. I. Krohn, G. Hermanson, A. Mallia, F. Gartner, M. Provenzano, E. Fujimoto, N. Goeke, B. Olson and D. Klenk, Anal. Biochem., 1985, **150**, 76.

38 S. A. James, B. N. Feltis, M. D. de Jonge, M. Sridhar, J. A. Kimpton, M. Altissimo, S. Mayo, C. Zheng, A. Hastings, D. L. Howard, D. J. Paterson, P. F. A. Wright, G. F. Moorhead, T. W. Turney and J. Fu, ACS Nano, 2013, **7**, 10621.

39 H. Otsuka, Y. Nagasaki and K. Kataoka, Adv. Drug Deliv. Rev., 2012, **64**, 246.

40 Z. Liu, J. T. Robinson, X. M. Sun and H. J. Dai, J. Am. Chem. Soc., 2008, **130**, 10876.

41 M. Yamaura, R. L. Camilo, L. C. Sampaio, M. A. Macêdo, M. Nakamura and H. E. Toma, J. Magn. Magn. Mater., 2004, **279**, 210.

42 H. Yin, P. S. Casey, M. J. McCall and M. Fenech, Langmuir, 2010, **26**, 15399.

43 M. Horie, K. Nishio, K. Fujita, S. Endoh, A. Miyauchi, Y. Saito, H. Iwahashi, K. Yamamoto, H. Murayama, H. Nakano, N. Nanashima, E. Niki and Y. Yoshida, Chem. Res. Toxicol., 2009, **22**, 543.

44 J. R. Casey, S. Grinstein and J. Orlowski, Nat. Rev. Mol. Cell Bio., 2010, **11**, 50.

45 V. Wilhelmi, U. Fischer, H. Weighardt, K. Schulze-Osthoff, C. Nickel, B. Stahlmecke, T. A. Kuhlbusch, A. M. Scherbart, C. Esser, R. P. Schins and C. Albrecht, PLoS One, 2013, **8**, e65704, doi:10.1371/journal.pone.0065704.

46 L. M. Canzoniero, D. M. Turetsky and D. W. Choi, J. Neurosci., 1999, **19**, RC31.

47 G. J. Doherty and H. T. McMahon, Annu. Rev. Biochem., 2009, **78**, 857.

48 A. Salvati, A. S. Pitek, M. P. Monopoli, K. Prapainop, F. B. Bombelli, D. R. Hristov, P. M. Kelly, C. Aberg, E. Mahon and K. A. Dawson, Nat. Nanotechnol., 2013, 8, 137.

49 S. Tenzer, D. Docter, J. Kuharev, A. Musyanovych, V. Fetz, R. Hecht, F. Schlenk, D. Fischer, K. Kiouptsi, C. Reinhardt, K. Landfester, H. Schild, M. Maskos, S. K. Knauer and R. H. Stauber, Nat. Nanotechnol., 2013, **8**, 772.

50. M. P. Monopoli, C. Åberg, A. Salvati and K. A. Dawson, Nat. Nanotechnol., 2012, **7**, 779-786.

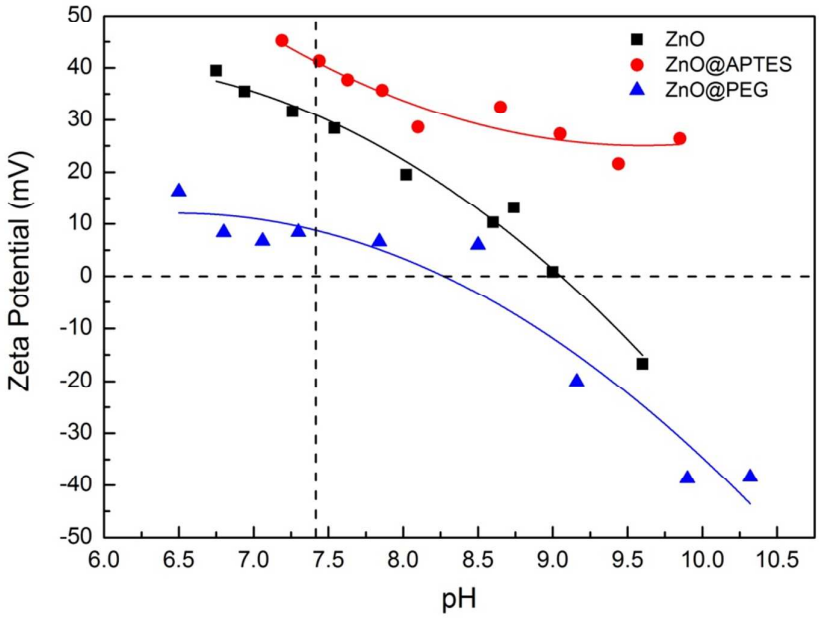

Figure 1. Zeta potential of bare and surface modified ZnO NPs in water with different pH.

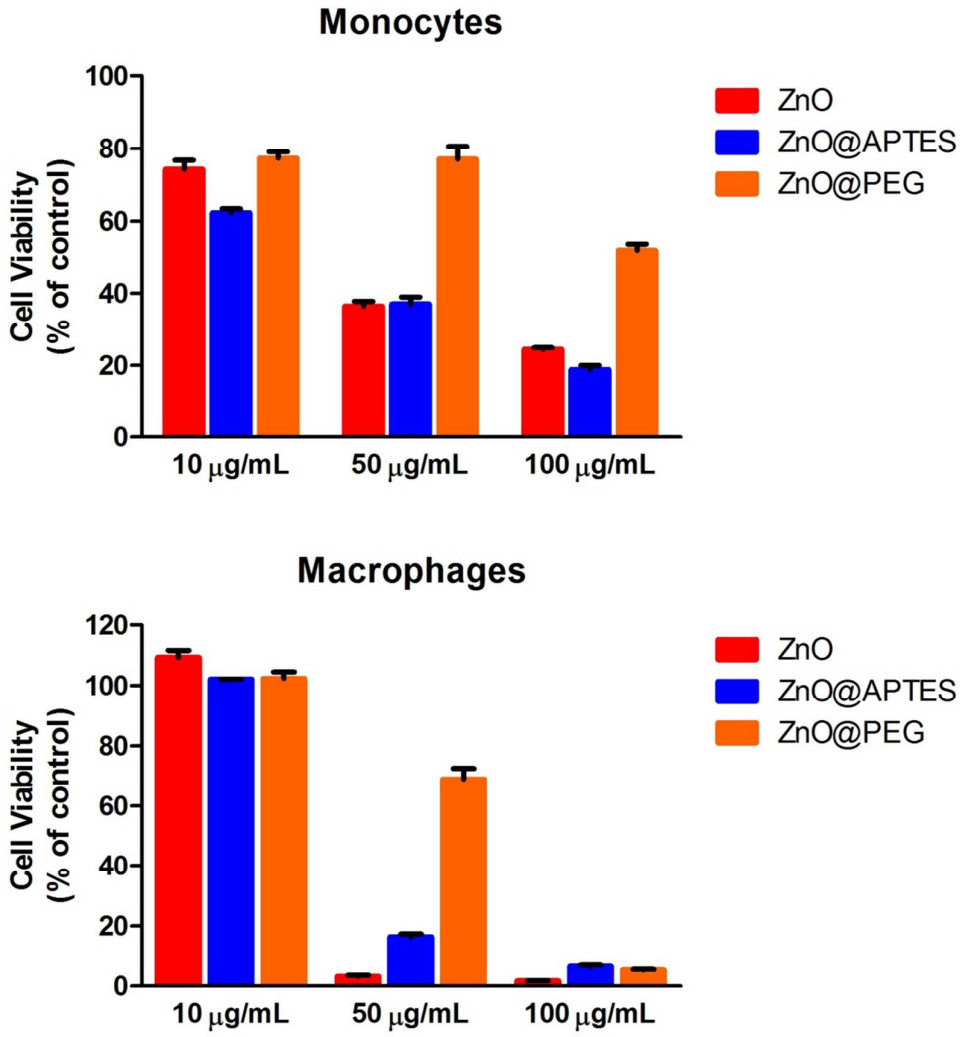

Figure 2. Cell viability of human THP-1 monocytes (A) and macrophages (B) after 24 h exposure to bare or surface modified ZnO NPs (mean ± SE, n=3 experiments).

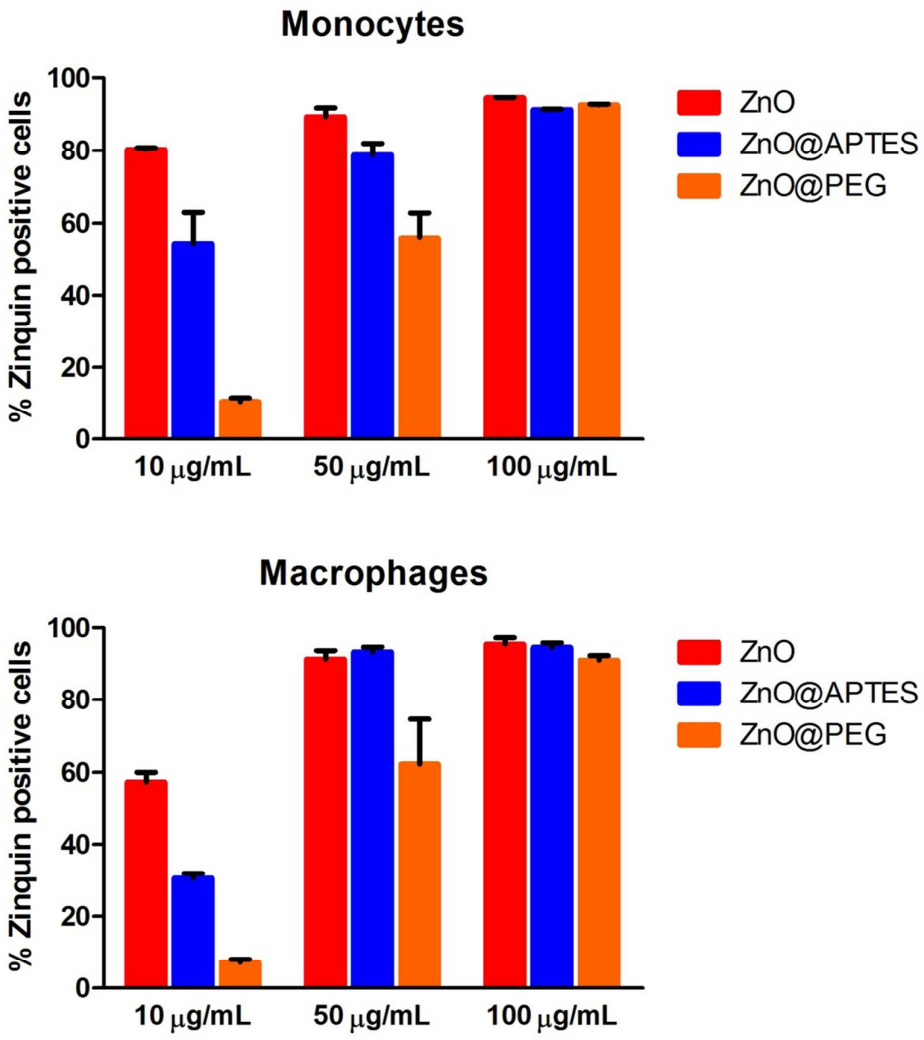

Figure 3. Percentage of monocytes (A) and macrophages (B) containing high levels of zinc ions after 24 h exposure to bare or surface modified ZnO NPs, relative to the endogenous available zinc in untreated (control) cells (mean ± SEM, n=3 experiments).

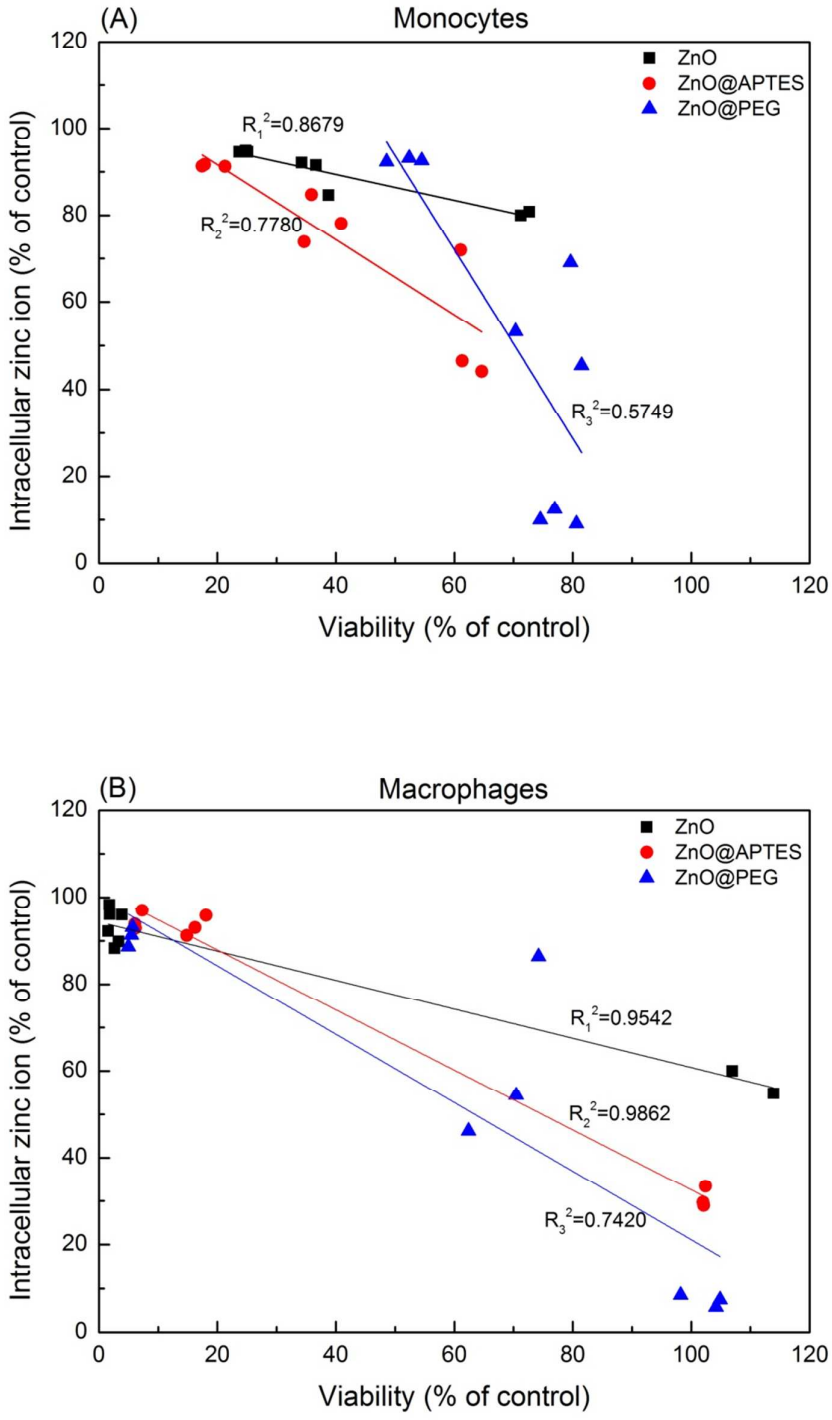

Figure 4. Inter-correlation of cell viability and intracellular zinc levels for ZnO NP-treated THP-1 monocytes (A) and macrophages (B).

Table 1. Total cell-associated Zn concentrations determined by ICP-MS

Material and concentration	Mass of zinc in monocytes (pg/cell[a])	Mass of zinc in macrophages (pg/cell[a])
Untreated cells	n.d.[b]	n.d.[b]
ZnO; 50 µg/mL	15.87±0.42	25.33±2.84
ZnO@APTES; 50 µg/mL	15.42±2.59	29.93±3.53
ZnO@PEG; 50 µg/mL	0.98±0.11	1.77±0.08

a. Cell populations per well were 100,000 both for monocytes and macrophages.

b. The concentration of zinc in untreated cells was below the instrument detection limit.

Table 2. Solubility of ZnO NPs in water, RPMI-1640 medium, medium with 10% v/v FBS and artificial lysosomal fluid (ALF) using ultracentrifugation

Material ([Zn] source) 100 µg/mL	Water (mM [%] in supernatant)	RPMI-1640 (mM [%] in supernatant)	RPMI-1640+FBS (mM [%] in supernatant)	ALF (mM [%] in supernatant)
1.28mM [Zn] (ZnO NPs)	0.0282±0.0016 [2.20%]	0.0251±0.0015 [1.96%]	0.0119±0.0012 [0.93%]	1.2561±0.0157 [98.13%]
1.28mM [Zn] (ZnO@APTES)	0.0287±0.0010 [2.24%]	0.0224±0.0012 [1.75%]	0.0089±0.0016 [0.69%]	1.2024±0.0187 [93.94%]
1.28mM [Zn] (ZnO@PEG)	0.0294±0.0009 [2.30%]	0.0215±0.0011 [1.68%]	0.0069±0.0022 [0.54%]	1.1752±0.0252 [91.82%]
1.28mM [Zn] ($ZnCl_2$)	1.0903±0.0221 [85.18%]	0.0257±0.0023 [2.01%]	0.0255±0.0191 [2.00%]	1.0418±0.0342 [81.39%]

Table 3. Zinc mass balance for 100 μg/mL ZnO NPs treated macrophages

Zinc mass flow	**ZnO [μM]**	**ZnO@APTES [μM]**	**ZnO@PEG [μM]**
Unreacted ZnO NPs	89.52% [1369±5]	89.08% [1362±2]	98.5% [1506±2]
Dissolved extracellular Zn	0.78% [11.9±1.2]	0.58% [8.9±0.8]	0.45% [6.9±0.7]
Intact intracellular ZnO NPs	9.46% [145±5]	10.15% [155±2]	0.86% [13.2±1.8]
Dissolved intracellular Zn	0.24% [3.7±0.8]	0.19% [2.9±0.3]	0.19% [2.9±0.2]

Table 4. Total protein-related Zn concentration determined by ICP-MS

Material and concentration	**Concentration of protein (μg/mL)**	**Concentration of zinc (μg/mL)**	**Protein/Zinc mass ratios**
ZnO; 2.5 mg/mL	758.6	88.7	8.6
ZnO@APTES; 2.5 mg/mL	1905.5	109.7	17.4
ZnO@PEG; 2.5 mg/mL	257.0	75.9	3.4